OL Organic Letters

pubs.acs.org/OrgLett

Letter

Enhancement of the Chiroptical Properties of *o*-OPE through Arene−Perfluoroarene Interactions

Published as part of Organic Letters special issue "π-Conjugated Molecules and Materials".

Darío Otero,[▽] Álvaro Martínez-Pinel,[▽] Ana M. Ortuño, Luis Álvarez de Cienfuegos, Juan M. Cuerva, Giovanna Longhi, Alba Millán,* and Delia Miguel*

Cite This: *Org. Lett.* 2025, 27, 8459−8463

Read Online

ACCESS | Metrics & More | Article Recommendations | Supporting Information

ABSTRACT: In this work, we synthesized and studied fluorinated *o*-oligophenylene ethynylenes (*o*-OPEs). Arene−perfluoroarene interactions promote the folding of the extremes of the OPE stabilizing folded conformations and extending the helical conformation to two complete turns, thus improving their chiroptical responses compared to the nonfluorinated analogue. Dissymmetry factors g_{abs} and g_{lum} reached values of ∼3 × 10^{-2} on the perfluorinated compound, which represents a 3-fold increase compared to that of the nonfluorinated analogue and is an exceptional value for a small organic molecule.

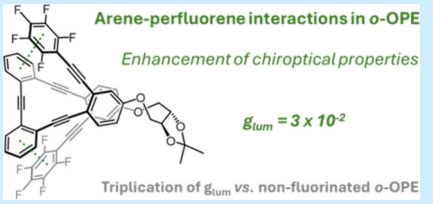

The development of CPL-emitting compounds has experienced exponential growth during the past decade,[1] due to the promising applications they have in fields as diverse as asymmetric synthesis,[2−6] chiroptical sensing,[7−9] chiral optoelectronics,[10] information sciences, and anticounterfeiting devices.[11−13] The quantification parameter of CPL is the luminescence dissymmetry factor (g_{lum}), which is determined by the equation $g_{lum} = 2 \times (I_L - I_R)/(I_L + I_R)$, where I_L and I_R are defined as the intensity of left- and right-handed circularly polarized light, respectively. To date, many strategies have been developed to improve the g_{lum} value, including supramolecular assembly of chiral materials[14,15] and the optimization of simple organic molecules,[16−18] among others.

Concerning this last approach, during the past several years, our group has been involved in the optimization of the chiroptical properties of helical scaffolds based on the *o*-oligophenylene ethynylene (*o*-OPE) skeleton.[19−22] In this sense, we described chiral stapling as an efficient way to induce a fixed helical sense in the structure, allowing the preparation of ratiometric probes in the ground and excited states.[23] With this strategy, we have prepared systems with up to four complete turns,[20] where a linear relationship between the magnetic dipole transition moment and the length of the helix was observed. However, dissymmetry factor g_{lum} did not follow a trend, suggesting that the helical chirality was lost when the distance to the chiral nucleus increased due to the flexibility of the structures. Although coordination with carbophilic metals as Ag(I) favors folding, this effect is partial and involves a substantial quenching of the fluorescence, reducing the applications based on CPL. To overcome this issue, in this work we aim to introduce substituents that promote an enhancement of noncovalent interactions. This fact would facilitate the folding of the structure without the need to use metals. Within this context, aromatic and perfluoroaromatic compounds present opposite quadrupoles derived from the large difference in electronegativity between the hydrogen and fluorine atoms, thus favoring an interaction between them due to an enthalpically favorable stacking,[24−26] which can also be affected by Pauli repulsion and dispersion interactions.[24,25,27] The strength of these arene−perfluoroarene π−π interactions has been proved in the oligomer conformation of *p*-phenylene ethynylene derivatives[28] and in the folding of macrocycles based on *o*-phenylenes.[29] In addition, these interactions have been recently exploited to promote peptide folding by force-driven clamping[30] and two-dimensional peptide assembly,[31] to hierarchically build supramolecular chirality,[32] to induce chiroptical inversion and precise ee detection of chiral acids,[33] and to promote CPL switching[34] and amplification,[35] among others.[36]

Herein, we have designed three fluorinated compounds, (*S*,*S*,*P*)-**1**-F_1, (*S*,*S*,*P*)-**1**-F_3, and (*S*,*S*,*P*)-**1**-F_5, that are two-turn helix analogues to our previously described nonfluorinated (*S*,*S*,*P*)-**1**.[20] The fluorine atoms have been introduced into the benzene rings at both ends of the helix (Figure 1). Our working hypothesis states that the inclusion of fluorine atoms would improve the folding of the structure with respect to (*S*,*S*,*P*)-**1** (73.6% folded as shown by DFT calculations) and consequently the g_{lum} value. This increase in the chiroptical

Received: June 5, 2025
Revised: July 12, 2025
Accepted: July 28, 2025
Published: July 30, 2025

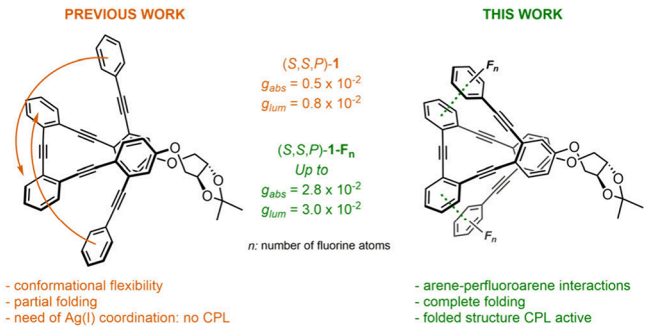

Figure 1. Working hypothesis and structure of enantiopure (*S,S,P*)-**1**-$\mathbf{F}_n$.

response, together with the preservation of the fluorescent quantum yield, would afford an improved candidate for CPL applications.

The synthesis of enantiopure compounds (*S,S,P*)-**1**-$\mathbf{F}_n$ (n = 1, 3, or 5) was carried out following our previously described methodology.[20] Thus, Sonogashira cross-coupling reactions between enantiopure brominated core (*S,S,P*)-**I** and corresponding alkynes **II**-$\mathbf{F}_n$ afforded the final products in good yields (Scheme 1). Likewise, enantiomers (*R,R,M*)-**1**-$\mathbf{F}_n$ were prepared from (*R,R,M*)-**I**.

Scheme 1. Synthesis of (*S,S,P*)-1-$\mathbf{F}_n$

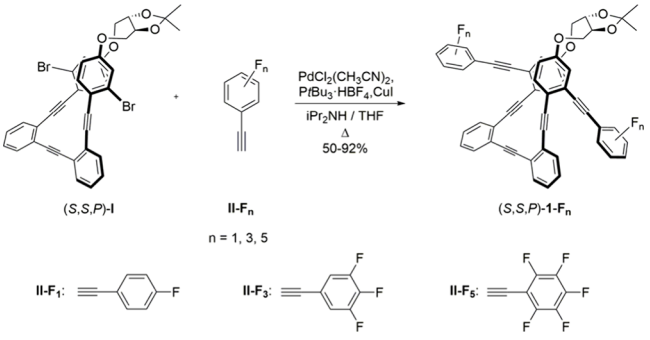

With the three pairs of enantiomers in hand, we evaluated their photophysical and chiroptical properties. First, we studied the photophysical properties of (*S,S,P*) enantiomers in CH_2Cl_2 solutions (Figure 2, left panels). All three compounds, (*S,S,P*)-**1**-$\mathbf{F}_1$, (*S,S,P*)-**1**-$\mathbf{F}_3$, and (*S,S,P*)-**1**-$\mathbf{F}_5$, presented similar absorbance and emission spectra. The compounds presented absorbance maxima at 274, 282, and 279 nm, respectively, with a shoulder centered at 340 nm in all cases (Figure 2, central panels). Fluorescence spectra showed a single peak with a maximum at ca. 423 nm with similar values of fluorescence quantum yield for the three derivatives (30%, 20%, and 21%, respectively), which were in the range of, or higher than, that observed for (*S,S,P*)-**1** (19%).[20] To shed light on the effect of fluorine atoms on the electronic characteristics of the OPEs, we explored the influence of the solvent nature on the photophysical properties of (*S,S,P*)-**1**-$\mathbf{F}_5$. Both the absorbance and the emission were comparable in different solvents (Figure S10), ranging from apolar (hexane) to polar ones, including protic (MeOH) and aprotic (MeCN) solvents. Fluorescence decay curves fitted to a biexponential function in all cases (Table S1), the average lifetime being around 4 ns in all of the solvents.[20] Concerning fluorescence quantum yields (QYs), small differences were observed, the highest value being in CH_2Cl_2 (21%) and the lowest in MeOH (16%) (Table S1).[20] The behavior of mono- and trifluorinated derivatives was also analyzed in these edge cases. In both solvents, a decrease in the QY was observed with an increase in the number of fluorine substituents, but there were no significant changes in the fluorescence lifetime values. On the other hand, as for the case of (*S,S,P*)-**1**-$\mathbf{F}_5$, similar differences were observed for each compound between solvents. This suggests that these properties are independent of the environment, thus supporting structural robustness.

Next, we investigated the chiroptical responses of the three enantiomeric pairs (*S,S,P*)/(*R,R,M*)-**1**-$\mathbf{F}_1$, (*S,S,P*)/(*R,R,M*)-**1**-$\mathbf{F}_3$, and (*S,S,P*)/(*R,R,M*)-**1**-$\mathbf{F}_5$ in CH_2Cl_2 solutions (Figure 2, right). The similarities in the ECD spectra of (*S,S,P*)-$\mathbf{F}_n$ compared to those obtained for nonfluorinated (*S,S,P*)-**1**[20] (Figure S11a) revealed that the previously observed *P* helicity is maintained. For the first transition, an increase in the maximum ECD signal together with a bathochromic shift was observed from (*S,S,P*)-**1**-$\mathbf{F}_1$ ($\Delta\varepsilon$ = 23.7 M^{-1} cm^{-1} at 375 nm) to (*S,S,P*)-**1**-$\mathbf{F}_3$ ($\Delta\varepsilon$ = 54.7 M^{-1} cm^{-1} at 387 nm). For (*S,S,P*)-**1**-$\mathbf{F}_5$, the wavelength of the maxima was quite similar to that of (*S,S,P*)-**1**-$\mathbf{F}_3$, but a lower ECD value was obtained ($\Delta\varepsilon$ = 30.4 M^{-1} cm^{-1} at 385 nm), which was consistent with the lower values of molar absorptivity. Regarding CPL spectra, a direct relationship between the number of fluorine atoms and the CPL signal was observed, reaching a maximum value for the perfluorinated derivative.

In addition, we measured the ECD and CPL of (*S,S,P*)-**1**-$\mathbf{F}_5$ and (*R,R,M*)-**1**-$\mathbf{F}_5$ solutions in the previously mentioned solvents. Concerning ECD, small differences were observed, affording slightly higher intensities in the most polar solvents (Figure S13a). Thus, in a MeCN solution, the less energetic band, which displayed a positive Cotton effect, presents a $\Delta\varepsilon$ value of 34.3 M^{-1} cm^{-1} at 385 nm. The comparison of the emission properties led us to similar conclusions. As one can see in the CPL spectra (Figure S13b), both the shape and the intensity were almost identical, showing no significant influence of the solvent on the excited state of the molecule.

Finally, to shed light on the impact of the fluorine atoms on chiroptical properties, we measured the absorption and luminescence dissymmetry factors (g_{abs} and g_{lum}, respectively) of all (*S,S,P*) enantiomers. As one can see in Table 1, absolute values increased with the number of fluorine atoms compared to those of nonfluorinated derivative (*S,S,P*)-**1**.[20] Specifically, the introduction of one ((*S,S,P*)-**1**-$\mathbf{F}_1$) and three ((*S,S,P*)-**1**-$\mathbf{F}_3$)) fluorine atoms into the outermost benzene rings led to 13% and 140% increases in g_{abs} and 12.5% and 75% increases in g_{lum}, respectively. This enhancement is much more prominent in (*S,S,P*)-**1**-$\mathbf{F}_5$, where arene−perfluoroarene interactions are maximized by the introduction of five fluorine atoms. In this case, the chiroptical response is boosted to nearly 4 times its original value. For this compound, we also obtained very similar g_{lum} values in all of the solvents (see the Supporting Information), suggesting the stability of the structure is independent of the environment.

This fact highlights the strength of the $\pi-\pi$ interactions between the arene and perfluoroarene rings when five fluorine atoms are present. It is noteworthy that the g_{abs} magnitude increases more than 5-fold with respect to (*S,S,P*)-**1** and is even better than that obtained in the folded (*S,S,P*)-**1**:Ag(I) complex (2.5×10^{-2}).[20] This demonstrates that the structure is completely folded in solution. To provide further evidence, we carried out ECD titrations of compounds (*S,S,P*)-**1**-$\mathbf{F}_n$,

https://doi.org/10.1021/acs.orglett.5c02277
Org. Lett. 2025, 27, 8459−8463

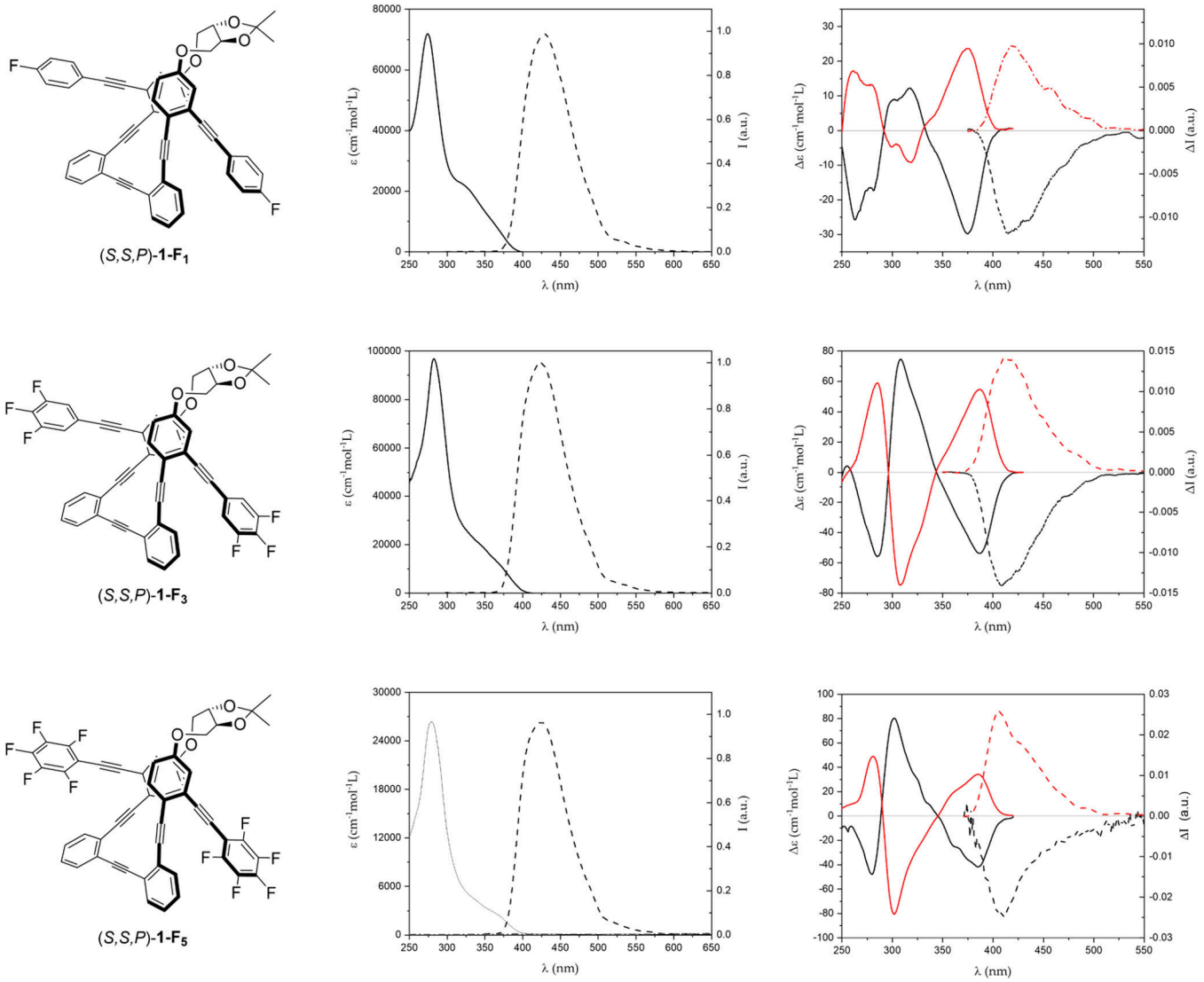

Figure 2. Structures (left) of (*S,S,P*)-**1**-F_1 (top), (*S,S,P*)-**1**-F_3 (middle), and (*S,S,P*)-**1**-F_5 (bottom). UV−vis (solid line) and fluorescence (dashed line) spectra (center) of (*S,S,P*)-**1**-F_n. ECD (solid line) and CPL (dashed line) (right) of (*S,S,P*)-**1**-F_n (red line) and (*R,R,M*)-**1**-F_n (black line). All of the spectra were recorded using 1.5×10^{-5} M solutions in CH_2Cl_2.

Table 1. g_{abs} and g_{lum} Values of Fluorinated *o*-OPEs in CH_2Cl_2

compound	g_{abs} (λ (nm))	g_{lum} (λ (nm))
(*S,S,P*)-**1**	0.45×10^{-2} (387)	0.8×10^{-2} (402)
(*S,S,P*)-**1**-F_1	0.51×10^{-2} (376)	0.9×10^{-2} (406)
(*S,S,P*)-**1**-F_3	1.2×10^{-2} (387)	1.4×10^{-2} (400)
(*S,S,P*)-**1**-F_5	2.8×10^{-2} (389)	3×10^{-2} (398)

adding increasing quantities of Ag(I) without changing the ligand concentration. As depicted in Figure S19, the behavior of extreme cases (*S,S,P*)-**1** and (*S,S,P*)-**1**-F_5 is quite different. For (*S,S,P*)-**1**-F_5, no significant change in the last band after the metal addition was obtained, demonstrating again that the folding is not dependent on the coordination. For mono- and trifluorinated derivatives, we observed an intermediate evolution of the ECD signal.

To rationalize observed dissymmetry ratios g_{abs} and g_{lum} and their increase upon fluorination, DFT calculations have been performed. One must be aware, however, of the difficulties for such approach in adequately representing arene−perfluoroarene $\pi-\pi$ interactions, where the interplay of Pauli repulsion, dispersion interactions, and electrostatics has a role. We considered in detail the two cases (*S,S,P*)-**1** and (*S,S,P*)-**1**-F_5, performed a conformational search, and optimized the structures (Supporting Information). In both cases, a folded structure, stabilized by $\pi-\pi$ interactions, is by far the lowest-energy one (conformer "a" (Tables S2 and S3)). Conformers are described by the reciprocal orientation of the phenylene ethynylene moieties ($\tau_1-\tau_3$ angles) and by conformational degrees of freedom of the chiral staple, which are responsible for the stabilization of the (*S,S,P*) form. At the adopted level of calculations, the first "unfolded" structure found for (*S,S,P*)-**1**-F_5 (conformer "f" (Table S2)) is 5.12 kcal/mol higher in energy above the most stable one, while the first "unfolded" structure found for (*S,S,P*)-**1** (conformer "f", Table S3) is only 0.74 kcal/mol higher than the lowest-energy structure. It should be noted that while the unfolded structure is not populated at all in (*S,S,P*)-**1**-F_5, it represents 21% for (*S,S,P*)-**1**, being the second one in energy over the folded one. With the aim of comparing folded and unfolded geometries, we calculated the difference in energy also for (*S,S,P*)-**1**-F_1 (1.5

https://doi.org/10.1021/acs.orglett.5c02277
Org. Lett. 2025, 27, 8459−8463

kcal/mol) and (*S,S,P*)-**1**-F_3 (2.66 kcal/mol). It appears that fluorine atoms help in stabilizing the folded structure, as expected. Also, the trend observed on the calculated distance between terminal arenes progressively decreases with an increase in the number of fluorine atoms (Figure S21 and Table S5). Comparing calculated CD spectra, the most stable conformer does not show significant differences among the four examined compounds, attributing the observed spectroscopic differences to varying degrees of conformational disorder. The calculated CD spectrum of the first unfolded conformer shows in all cases a positive, weak, lowest-energy band, while the main differences are observed at 300 nm with a low-intensity band of opposite sign with respect to the stable folded structure. These theoretical results help to explain why the solvent dependence of CD signals is observed particularly in this spectroscopic region for compound (*S,S,P*)-**1** (Figure S12),[20] which lacks the stabilization effect of fluorine atoms, and not for (*S,S,P*)-**1**-F_5 (Figure S13a). Furthermore, the unfolded structure presents a higher absorbance in the 350−400 nm region that contributes to giving a lower g_{abs} value for (*S,S,P*)-**1** with respect to (*S,S,P*)-**1**-F_5 (Figure S25).

Finally, the CPL brightness (B_{CPL}) has been defined as an important parameter in chiroptical materials, as it includes information relative to both chirality and luminescence.[37] For (*S,S,P*)-**1**-F_5, B_{CPL} reaches 82 M^{-1} cm^{-1}, making this scaffold an outstanding candidate for chiroptical applications.

In conclusion, we synthesized three enantiomeric pairs of *o*-OPEs with an increasing number of fluorine atoms. Although they presented almost identical photophysical properties, striking differences were observed in their chiroptical responses. The introduction of one ((*S,S,P*)-**1**-F_1), three ((*S,S,P*)-**1**-F_3), and five ((*S,S,P*)-**1**-F_5) fluorine atoms into both outermost benzene rings led to 1.12-, 1.75-, and almost 4-fold increases, respectively, in g_{lum}. This enhancement is related to the stabilization of the helical arrangement by greater arene−perfluorarene interactions taking place with an increasing number of F atoms. The exceptional magnitude of g_{lum} found for (*S,S,P*)-**1**-F_5 together with the adequate value of quantum yield makes this simple organic molecule a promising scaffold as a model for CPL applications.

■ ASSOCIATED CONTENT

Data Availability Statement

The data underlying this study are available in the published article and its Supporting Information.

Supporting Information

The Supporting Information is available free of charge at https://pubs.acs.org/doi/10.1021/acs.orglett.5c02277.

Synthetic procedures and characterization of compounds, copies of NMR spectra, additional ECD and CPL spectra, lifetimes and QYs, theoretical calculation detailss and conformer analyses (PDF)

■ AUTHOR INFORMATION

Corresponding Authors

Alba Millán − *Departamento de Química Orgánica, Unidad de Excelencia de Química (UEQ), C. U. Fuentenueva, Universidad de Granada, 18071 Granada, Spain;* orcid.org/0000-0003-2754-270X; Email: amillan@ugr.es

Delia Miguel − *Departamento de Fisicoquímica, UEQ, Facultad de Farmacia, C. U. Cartuja, Universidad de Granada, 18071 Granada, Spain;* orcid.org/0000-0002-7876-3986; Email: dmalvarez@ugr.es

Authors

Darío Otero − *Departamento de Química Orgánica, Unidad de Excelencia de Química (UEQ), C. U. Fuentenueva, Universidad de Granada, 18071 Granada, Spain*

Álvaro Martínez-Pinel − *Departamento de Química Orgánica, Unidad de Excelencia de Química (UEQ), C. U. Fuentenueva, Universidad de Granada, 18071 Granada, Spain*

Ana M. Ortuño − *Departamento de Química Orgánica, Unidad de Excelencia de Química (UEQ), C. U. Fuentenueva, Universidad de Granada, 18071 Granada, Spain*

Luis Álvarez de Cienfuegos − *Departamento de Química Orgánica, Unidad de Excelencia de Química (UEQ), C. U. Fuentenueva, Universidad de Granada, 18071 Granada, Spain;* orcid.org/0000-0001-8910-4241

Juan M. Cuerva − *Departamento de Química Orgánica, Unidad de Excelencia de Química (UEQ), C. U. Fuentenueva, Universidad de Granada, 18071 Granada, Spain;* orcid.org/0000-0001-6896-9617

Giovanna Longhi − *Department of Molecular and Translational Medicine, Università di Brescia, 25121 Brescia, Italy; Istituto Nazionale di Ottica (INO), CNR, Research Unit of Brescia, 25123 Brescia, Italy;* orcid.org/0000-0002-0011-5946

Complete contact information is available at: https://pubs.acs.org/10.1021/acs.orglett.5c02277

Author Contributions

[▽]D.O. and Á.M.-P. contributed equally to this work.

Notes

The authors declare no competing financial interest.

■ ACKNOWLEDGMENTS

This work received financial support from Grants PID2023-146801NB-C31 and PID2021-127964NB-C22 funded by MICIU/AEI/10.13039/501100011033 and ERDF, EU. A.M.O. and Á.M.-P. acknowledge their FPU contracts (FPU16/02597 and FPU19/03751) funded by MCIN/AIE/10.13039/501100011033. Funding was provided also by the Italian Ministry of University and Research (MUR) (Project SMART HELIX, prot. 2022B3EFJH). Funding for open access charge: Universidad de Granada/CBUA.

■ REFERENCES

(1) Uceda, R. G.; Miguez-Lago, S.; M. Cruz, C.; P. Morcillo, S.; Álvarez de Cienfuegos, L.; Blanco, V.; G. Campaña, A.; Ribagorda, M.; Miguel, D.; M. Cuerva, J. Do's and Don'ts When Visiting Circularly Polarized Luminescence. *chemRxiv* **2025**, DOI: 10.26434/chemrxiv-2025-tqz5g-v2.

(2) Vega-Peñaloza, A.; Mateos, J.; Companyó, X.; Escudero-Casao, M.; Dell'Amico, L. A Rational Approach to Organo-Photocatalysis: Novel Designs and Structure-Property Relationships. *Angew. Chem., Int. Ed.* **2021**, *60* (3), 1082−1097.

(3) He, C.; Li, Y. Absolute Asymmetric Synthesis Driven by Circularly Polarized Light. *Chin. Chem. Lett.* **2023**, *34* (8), 108077.

(4) Xu, L.; Wu, Y.; Gao, R.; Li, S.; Liu, N.; Wu, Z. Visible Helicity Induction and Memory in Polyallene toward Circularly Polarized

Luminescence, Helicity Discrimination, and Enantiomer Separation. *Angew. Chem., Int. Ed.* **2023**, *62* (13), e202217234 DOI: 10.1002/anie.202217234.
(5) Zheng, W.; Oki, K.; Saha, R.; Hijikata, Y.; Yashima, E.; Ikai, T. One-Handed Helical Tubular Ladder Polymers for Chromatographic Enantioseparation. *Angew. Chem., Int. Ed.* **2023**, *62* (11), e202218297 DOI: 10.1002/anie.202218297.
(6) Han, D.; Yang, X.; Han, J.; Zhou, J.; Jiao, T.; Duan, P. Sequentially Amplified Circularly Polarized Ultraviolet Luminescence for Enantioselective Photopolymerization. *Nat. Commun.* **2020**, *11* (1), 5659.
(7) You, J.; Yin, C.; Wang, S.; Wang, X.; Jin, K.; Wang, Y.; Wang, J.; Liu, L.; Zhang, J.; Zhang, J. Responsive Circularly Polarized Ultralong Room Temperature Phosphorescence Materials with Easy-to-Scale and Chiral-Sensing Performance. *Nat. Commun.* **2024**, *15* (1), 7149.
(8) Jhun, B. H.; Park, S. Y.; You, Y. Molecular Sensors Producing Circularly Polarized Luminescence Responses. *Dyes Pigm.* **2023**, *208*, 110786.
(9) Carr, R.; Evans, N. H.; Parker, D. Lanthanide Complexes as Chiral Probes Exploiting Circularly Polarized Luminescence. *Chem. Soc. Rev.* **2012**, *41* (23), 7673.
(10) Zhang, D.-W.; Li, M.; Chen, C.-F. Recent Advances in Circularly Polarized Electroluminescence Based on Organic Light-Emitting Diodes. *Chem. Soc. Rev.* **2020**, *49* (5), 1331−1343.
(11) Liu, D.; Xiong, L.; Dong, X.; Han, Z.; Liu, H.; Zang, S. Reversible Local Protonation-Deprotonation: Tuning Stimuli-Responsive Circularly Polarized Luminescence in Chiral Hybrid Zinc Halides for Anti-Counterfeiting and Encryption. *Angew. Chem., Int. Ed.* **2024**, *63* (46), e202410416 DOI: 10.1002/anie.202410416.
(12) López-Sicilia, I.; Ortuño, A. M.; Reine, P.; Otero, D.; Martín-Romero, M. T.; Camacho, L.; Álvarez de Cienfuegos, L.; Orte, A.; Giner-Casares, J. J.; Miguel, D.; Cuerva, J. M. 2D Self-Assembly of o -OPE Foldamers for Chiroptical Barcoding. *J. Mater. Chem. C* **2023**, *11* (7), 2591−2599.
(13) Yang, N.; Zhao, J.; Liu, W.; Li, Y.; Yang, Y. Cholesteric Liquid Crystal Polymer Networks Doped with an Axially Chiral Fluorescent Dye: Circularly Polarized Luminescence and Anti-Counterfeiting Applications. *Adv. Opt. Mater.* **2025**, *13* (2), 2402128 DOI: 10.1002/adom.202402128.
(14) He, S.; Jiang, Z.; Dou, X.; Gao, L.; Feng, C. Chiral Supramolecular Assemblies: Controllable Construction and Biological Activity. *ChemPlusChem* **2023**, *88* (7), e202300226 DOI: 10.1002/cplu.202300226.
(15) Ariga, K.; Mori, T.; Kitao, T.; Uemura, T. Supramolecular Chiral Nanoarchitectonics. *Adv. Mater.* **2020**, *32* (41), 1905657 DOI: 10.1002/adma.201905657.
(16) Sánchez-Carnerero, E. M.; Agarrabeitia, A. R.; Moreno, F.; Maroto, B. L.; Muller, G.; Ortiz, M. J.; de la Moya, S. Circularly Polarized Luminescence from Simple Organic Molecules. *Chem. - Eur. J.* **2015**, *21* (39), 13488−13500.
(17) Wang, Y.; Gong, J.; Wang, X.; Li, W.; Wang, X.; He, X.; Wang, W.; Yang, H. Multistate Circularly Polarized Luminescence Switching through Stimuli-Induced Co-Conformation Regulations of Pyrene-Functionalized Topologically Chiral [2]Catenane. *Angew. Chem., Int. Ed.* **2022**, *61* (44), e202210542 DOI: 10.1002/anie.202210542.
(18) Zhang, X.; Liu, H.; Zhuang, G.; Yang, S.; Du, P. An Unexpected Dual-Emissive Luminogen with Tunable Aggregation-Induced Emission and Enhanced Chiroptical Property. *Nat. Commun.* **2022**, *13* (1), 3543.
(19) Resa, S.; Miguel, D.; Guisán-Ceinos, S.; Mazzeo, G.; Choquesillo-Lazarte, D.; Abbate, S.; Crovetto, L.; Cárdenas, D. J.; Carreño, M. C.; Ribagorda, M.; Longhi, G.; Mota, A. J.; Álvarez de Cienfuegos, L.; Cuerva, J. M. Sulfoxide-Induced Homochiral Folding of Ortho -Phenylene Ethynylenes (o -OPEs) by Silver(I) Templating: Structure and Chiroptical Properties. *Chem. - Eur. J.* **2018**, *24* (11), 2653−2662.
(20) Ortuño, A. M.; Reiné, P.; Resa, S.; Álvarez de Cienfuegos, L.; Blanco, V.; Paredes, J. M.; Mota, A. J.; Mazzeo, G.; Abbate, S.; Ugalde, J. M.; Mujica, V.; Longhi, G.; Miguel, D.; Cuerva, J. M. Extended Enantiopure Ortho -Phenylene Ethylene (o -OPE)-Based Helical Systems as Scaffolds for Supramolecular Architectures: A Study of Chiroptical Response and Its Connection to the CISS Effect. *Org. Chem. Front.* **2021**, *8* (18), 5071−5086.
(21) Reiné, P.; Ortuño, A. M.; Resa, S.; Álvarez de Cienfuegos, L.; Blanco, V.; Ruedas-Rama, M. J.; Mazzeo, G.; Abbate, S.; Lucotti, A.; Tommasini, M.; Guisán-Ceinos, S.; Ribagorda, M.; Campaña, A. G.; Mota, A.; Longhi, G.; Miguel, D.; Cuerva, J. M. OFF/ON Switching of Circularly Polarized Luminescence by Oxophilic Interaction of Homochiral Sulfoxide-Containing o -OPEs with Metal Cations. *Chem. Commun.* **2018**, *54* (99), 13985−13988.
(22) Reine, P.; Campaña, A. G.; Alvarez de Cienfuegos, L.; Blanco, V.; Abbate, S.; Mota, A. J.; Longhi, G.; Miguel, D.; Cuerva, J. M. Chiral Double Stapled o -OPEs with Intense Circularly Polarized Luminescence. *Chem. Commun.* **2019**, *55* (72), 10685−10688.
(23) Reiné, P.; Justicia, J.; Morcillo, S. P.; Abbate, S.; Vaz, B.; Ribagorda, M.; Orte, Á.; Álvarez de Cienfuegos, L.; Longhi, G.; Campaña, A. G.; Miguel, D.; Cuerva, J. M. Pyrene-Containing Ortho -Oligo(Phenylene)Ethynylene Foldamer as a Ratiometric Probe Based on Circularly Polarized Luminescence. *J. Org. Chem.* **2018**, *83* (8), 4455−4463.
(24) Lee, G. Y.; Hu, E.; Rheingold, A. L.; Houk, K. N.; Sletten, E. M. Arene-Perfluoroarene Interactions in Solution. *J. Org. Chem.* **2021**, *86* (12), 8425−8436.
(25) Zhang, S.; Chen, A.; An, Y.; Li, Q. Arene-Perfluoroarene Interaction: Properties, Constructions, and Applications in Materials Science. *Matter* **2024**, *7* (10), 3317−3350.
(26) Schramm, B.; Gray, M.; Herbert, J. M. Substituent and Heteroatom Effects on $\pi-\pi$ Interactions: Evidence That Parallel-Displaced π-Stacking Is Not Driven by Quadrupolar Electrostatics. *J. Am. Chem. Soc.* **2025**, *147* (4), 3243−3260.
(27) Carter-Fenk, K.; Herbert, J. M. Electrostatics Does Not Dictate the Slip-Stacked Arrangement of Aromatic $\pi-\pi$ Interactions. *Chem. Sci.* **2020**, *11* (26), 6758−6765.
(28) Sharber, S. A.; Baral, R. N.; Frausto Arellano, F.; Haas, T. E.; Müller, P.; Thomas, S. W., III Substituent Effects That Control Conjugated Oligomer Conformation through Non-Covalent Interactions. *J. Am. Chem. Soc.* **2017**, *139* (14), 5164−5174.
(29) Kirinda, V. C.; Hartley, C. S. Folding-Controlled Assembly of Ortho -Phenylene-Based Macrocycles. *Chem. Sci.* **2021**, *12* (20), 6992−7002.
(30) Xu, Y.; Hao, A.; Xing, P. Dynamic Chiral Folding for Arene−Perfluoroarene Force Driven Clamping. *Nano Lett.* **2025**, *25* (17), 7128−7136.
(31) Kim, T.; Hong, J.; Kim, J.; Cho, J.; Kim, Y. Two-Dimensional Peptide Assembly via Arene−Perfluoroarene Interactions for Proliferation and Differentiation of Myoblasts. *J. Am. Chem. Soc.* **2023**, *145* (3), 1793−1802.
(32) Liang, J.; Zhang, H.; Hao, A.; Xing, P. Hierarchically Evolved Supramolecular Chirality Mediated by Arene-Perfluoroarene Interaction. *ACS Appl. Mater. Interfaces* **2021**, *13* (24), 29170−29178.
(33) Zhao, J.; Wang, B.; Hao, A.; Xing, P. Arene−Perfluoroarene Interaction Induced Chiroptical Inversion and Precise Ee% Detection of Chiral Acids in a Benzimidazole-Involved Ternary Coassembly. *Nanoscale* **2022**, *14* (5), 1779−1786.
(34) Gu, Z.; Ma, W.; Feng, J.; Liu, Z.; Xu, B.; Tian, W. Circularly Polarized Luminescence Switching Driven by Precisely Tuned Supramolecular Interactions: From Hydrogen Bonding to $\pi-\pi$ Interaction. *J. Phys. Chem. Lett.* **2023**, *14* (28), 6437−6443.
(35) Yang, S.; Li, F.; Li, Q.; Han, J.; Cheng, Y. Chiral Coassembly-Activated CPL Amplification Promoted by Electrostatic and Arene−Perfluoroarene Interactions. *ACS Appl. Opt. Mater.* **2023**, *1* (8), 1492−1500.
(36) Liu, B.; Gao, J.; Hao, A.; Xing, P. Arene-Perfluoroarene Force Driven Sublimation-Removable Chiral Coassemblies. *Angew. Chem., Int. Ed.* **2023**, *62* (25), e202305135 DOI: 10.1002/anie.202305135.
(37) Arrico, L.; Di Bari, L.; Zinna, F. Quantifying the Overall Efficiency of Circularly Polarized Emitters. *Chem. - Eur. J.* **2021**, *27* (9), 2920−2934.

https://doi.org/10.1021/acs.orglett.5c02277
Org. Lett. 2025, 27, 8459−8463